hydrolase activity of parkinsonism-associated human ubiquitin carboxyl-terminal hydrolase L1 variants. *Biochem. Biophys. Res. Commun.* **304**, 176-183.

Noctor, S. C., Flint, A. C., Weissman, T. A., Dammerman, R. S. and Kriegstein, A. R. (2001). Neurons derived from radial glial cells establish radial units in neocortex. *Nature* **409**, 714-720.

Noctor, S. C., Flint, A. C., Weissman, T. A., Wong, W. S., Clinton, B. K. and Kriegstein, A. R. (2002). Dividing precursor cells of the embryonic cortical ventricular zone have morphological and molecular characteristics of radial glia. *J. Neurosci.* **22**, 3161-3173.

Noctor, S. C., Martinez-Cerdeno, V., Ivic, L. and Kriegstein, A. R. (2004). Cortical neurons arise in symmetric and asymmetric division zones and migrate through specific phases. *Nat. Neurosci.* **7**, 136-144.

Ogawa, H., Ishiguro, K., Gaubatz, S., Livingston, D. M. and Nakatani, Y. (2002). A complex with chromatin modifiers that occupies E2F- and Myc-responsive genes in G0 cells. *Science* **296**, 1132-1136.

Osaka, H., Wang, Y. L., Takada, K., Takizawa, S., Setsuie, R., Li, H., Sato, Y., Nishikawa, K., Sun, Y. J., Sakurai, M. et al. (2003). Ubiquitin carboxy-terminal hydrolase L1 binds to and stabilizes monoubiquitin in neuron. *Hum. Mol. Genet.* **12**, 1945-1958.

Patrick, G. N., Zhou, P., Kwon, Y. T., Howley, P. M. and Tsai, L. H. (1998). p35, the neuronal-specific activator of cyclin-dependent kinase 5 (Cdk5) is degraded by the ubiquitin-proteasome pathway. *J. Biol. Chem.* **273**, 24057-24064.

Qian, X., Goderie, S. K., Shen, Q., Stern, J. H. and Temple, S. (1998). Intrinsic programs of patterned cell lineages in isolated vertebrate CNS ventricular zone cells. *Development* **125**, 3143-3152.

Qian, X., Shen, Q., Goderie, S. K., He, W., Capela, A., Davis, A. A. and Temple, S. (2000). Timing of CNS cell generation: a programmed sequence of neuron and glial cell production from isolated murine cortical stem cells. *Neuron* **28**, 69-80.

Qiu, L., Joazeiro, C., Fang, N., Wang, H. Y., Elly, C., Altman, Y., Fang, D., Hunter, T. and Liu, Y. C. (2000). Recognition and ubiquitination of Notch by Itch, a hect-type E3 ubiquitin ligase. *J. Biol. Chem.* **275**, 35734-35737.

Rice, D. S. and Curran, T. (2001). Role of the reelin signaling pathway in central nervous system development. *Annu. Rev. Neurosci.* **24**, 1005-1039.

Roegiers, F. and Jan, Y. N. (2004). Asymmetric cell division. *Curr. Opin. Cell Biol.* **16**, 195-205.

Saigoh, K., Wang, Y. L., Suh, J. G., Yamanishi, T., Sakai, Y., Kiyosawa, H., Harada, T., Ichihara, N., Wakana, S., Kikuchi, T. et al. (1999). Intragenic deletion in the gene encoding ubiquitin carboxy-terminal hydrolase in gad mice. *Nat. Genet.* **23**, 47-51.

Satoh, J. and Kuroda, Y. (2001). A polymorphic variation of serine to tyrosine at codon 18 in the ubiquitin C-terminal hydrolase-L1 gene is associated with a reduced risk of sporadic Parkinson's disease in a Japanese population. *J. Neurol. Sci.* **189**, 113-117.

Sauvageot, C. M. and Stiles, C. D. (2002). Molecular mechanisms controlling cortical gliogenesis. *Curr. Opin. Neurobiol.* **12**, 244-249.

Schofield, J. N., Day, I. N., Thompson, R. J. and Edwards, Y. H. (1995). PGP9.5, a ubiquitin C-terminal hydrolase; pattern of mRNA and protein expression during neural development in the mouse. *Brain Res. Dev. Brain Res.* **85**, 229-238.

Sekiguchi, S., Yoshikawa, Y., Tanaka, S., Kwon, J., Ishii, Y., Kyuwa, S., Wada, K., Nakamura, S. and Takahashi, K. (2003). Immunohistochemical analysis of protein gene product 9.5, a ubiquitin carboxyl-terminal hydrolase, during placental and embryonic development in the mouse. *Exp. Anim.* **52**, 365-369.

Shen, Q., Qian, X., Capela, A. and Temple, S. (1998). Stem cells in the embryonic cerebral cortex: their role in histogenesis and patterning. *J. Neurobiol.* **36**, 162-174.

Sullivan, M. L. and Vierstra, R. D. (1993). Formation of a stable adduct between ubiquitin and the Arabidopsis ubiquitin-conjugating enzyme, AtUBC1+. *J. Biol. Chem.* **268**, 8777-8780.

Tabata, H. and Nakajima, K. (2003). Multipolar migration: the third mode of radial neuronal migration in the developing cerebral cortex. *J. Neurosci.* **23**, 9996-10001.

Temple, S. (2001). The development of neural stem cells. *Nature* **414**, 112-117.

Weissman, A. M. (2001). Themes and variations on ubiquitylation. *Nat. Rev. Mol. Cell. Biol.* **2**, 169-178.

Wilkinson, K. D., Lee, K. M., Deshpande, S., Duerksen-Hughes, P., Boss, J. M. and Pohl, J. (1989). The neuron-specific protein PGP 9.5 is a ubiquitin carboxyl-terminal hydrolase. *Science* **246**, 670-673.

Zhong, W., Feder, J. N., Jiang, M. M., Jan, L. Y. and Jan, Y. N. (1996). Asymmetric localization of a mammalian numb homolog during mouse cortical neurogenesis. *Neuron* **17**, 43-53.

Zhong, W., Jiang, M. M., Weinmaster, G., Jan, L. Y. and Jan, Y. N. (1997). Differential expression of mammalian Numb, Numblike and Notch1 suggests distinct roles during mouse cortical neurogenesis. *Development* **124**, 1887-1897.

Exp. Anim. 55(1), 35–43, 2006

The Region-Specific Functions of Two Ubiquitin C-Terminal Hydrolase Isozymes along the Epididymis

Jungkee KWON[1, 3], Satoshi SEKIGUCHI[2], Yu-Lai WANG[1], Rieko SETSUIE[1], Yasuhiro YOSHIKAWA[2], and Keiji WADA[1]

[1]*Department of Degenerative Neurological Diseases, National Institute of Neuroscience, National Center of Neurology and Psychiatry, 4–1–1 Ogawahigashi, Kodaira, Tokyo 187-8502,*
[2]*Department of Biomedical Science, Graduate School of Agricultural and Life Sciences, The University of Tokyo, 1–1–1 Yayoi, Bunkyo-ku, Tokyo 113-8657, Japan, and*
[3]*Laboratory of Animal Medicine, College of Veterinary Medicine, Chonbuk National University, 664–14 Duckjin-Ku, Jeonju 561-756, Korea*

Abstract: *We previously showed that* gad *mice, which are deficient for ubiquitin C-terminal hydrolase L1 (UCH-L1), have a significantly increased number of defective spermatozoa, suggesting that UCH-L1 functions in sperm quality control during epididymal maturation. The epididymis is the site of spermatozoa maturation, transport and storage. Region-specific functions along the epididymis are essential for establishing the environment required for sperm maturation. We analyzed the region-specific expression of UCH-L1 and UCH-L3 along the epididymis, and also assessed the levels of ubiquitin, which has specificity for UCH-L1. In wild-type mice, western blot analysis demonstrated a high level of UCH-L1 expression in the caput epididymis, consistent with ubiquitin expression, whereas UCH-L3 expression was high in the cauda epididymis. We also investigated the function of UCH-L1 and UCH-L3 in epididymal apoptosis induced by efferent duct ligation. The caput epididymides of* gad *mice were resistant to apoptotic stress induced by efferent duct ligation, whereas* Uchl3 *knockout mice showed a marked increase in apoptotic cells following ligation. In conclusion, the response of* gad *and* Uchl3 *knockout mice to androgen withdrawal suggests a reciprocal function of the two UCH enzymes in the caput epididymis.*
Key words: *apoptosis, epididymis, ubiquitin, UCH*

Introduction

The mammalian epididymis is a highly convoluted tubule that connects the efferent ducts of the testis to the vas deferens [2, 8]. The epididymis is composed of three distinct compartments, caput (head), corpus (body) and cauda (tail), each having a specific role in sperm maturation, sustenance, transport, and storage [2, 6]. However, the molecular basis for the maturation process remains largely unknown.

It has been suggested that the epididymis acts as a quality control organ to eliminate defective spermato-

(Received 12 August 2005 / Accepted 4 November 2005)
Address corresponding: K. Wada, Department of Degenerative Neurological Diseases, National Institute of Neuroscience, National Center of Neurology and Psychiatry, 4–1–1 Ogawahigashi-cho, Kodaira, Tokyo 187-8502, Japan

zoa before ejaculation [37]. The epididymis is an organ with voluminous protein traffic between the epithelium and lumen. Numerous proteins, secreted in an apocrine manner by the epididymal epithelium, are implicated in spermatozoa maturation [18]. Two major components of the ubiquitin-dependent proteolytic pathway, ubiquitin and UCH-L1 (PGP9.5), are expressed in epididymal tissue [10, 35]. Ubiquitin is present in human seminal plasma [26], and defective spermatozoa become ubiquitinated during epididymal passage [23, 37]. Our previous work showed that UCH-L1 associates with monoubiquitin and stabilizes its expression [31]. In addition, it has been suggested that UCH-L1 functions as a regulator of apoptosis via the ubiquitin pathway [13, 23, 25]. We found that testes of gracile axonal dystrophy (*gad*) mice, which lack UCH-L1, have reduced ubiquitin levels and are resistant to cryptorchid injury–mediated germ cell apoptosis [25]. Furthermore, our recent work demonstrated that the percentage of morphologically abnormal spermatozoa is significantly higher in *gad* mice, compared with wild-type mice [23].

Two mouse UCH isozymes, UCH-L1 and UCH-L3, are strongly but reciprocally expressed in the testis during spermatogenesis [25], suggesting that these proteins have distinct functions in the testis [23], even though they have high amino acid sequence identity and share significant structural similarity [21]. The functional regionalization of the epididymis is delineated at the molecular level by regional differences in gene expression [16–19]. Regional differences along the epididymis might be essential characteristics of the environment required for sperm quality control. Although it has been shown that UCH-L1 and UCH-L3 have reciprocal functions with respect to cryptorchid injury, their molecular functions in regulating sperm quality during epididymal passage are not fully understood. Thus, we examined the epididymal expression of UCH-L1 and UCH-L3 with regard to their involvement in the regulation of apoptosis. In addition, we assessed the reciprocal functions of these two proteins in the epididymis.

Materials and Methods

Animals

We used *gad* (CBA/RFM) [34] and *Uchl3* knockout (C57BL/6J) [21] male mice at 10 weeks of age. The *gad* mouse is an autosomal recessive mutant that was obtained by crossing CBA and RFM mice. The *gad* line has been maintained by intercrossing for more than 20 generations [34]. *Uchl3* knockout mice were generated by the standard method [21] using homologously recombinant ES cells, and the knockout line has been back-crossed several times to C57BL/6J mice. Both strains are maintained at our institute. Animal care and handling were in accordance with our institutional regulations for animal care and were approved by the Animal Investigation Committee of the National Institute of Neuroscience, National Center of Neurology and Psychiatry.

Unilateral efferent duct ligation

Animals were either left intact to serve as controls or were unilaterally ligated at the efferent duct [9, 38]. Four mice in each group were anesthetized with pentobarbital (Abbott Laboratories, North Chicago, IL), and the testis and epididymis on the right side were exposed through a scrotal incision. The thin avascular attachment joining the initial segment of the epididymis to the tunica albuginea was cut to permit exposure of the efferent ducts coursing above and parallel to the vascular supply. A silk suture was passed by needle through the thin sheet of connective tissue between the ductules and the blood vessels, and the efferent ducts were occluded by ligation. Mice were sacrificed 2 or 4 days after ligation. Both epididymides were immersed in 4% paraformaldehyde for at least 24 hr before they were dehydrated and embedded in paraffin [22].

Histological and immunohistochemical assessment of the epididymis

The caput, corpus and cauda epididymides along the epididymal region embedded in paraffin were cut into 4-μm sections and stained with hematoxylin and eosin. Light microscopy was used for routine observations. For immunohistochemical staining, the sections were incubated with 10% goat serum for 1 h at room temperature followed by incubation overnight at 4°C with a rabbit polyclonal antibody raised against peptides within UCH-L1 or UCH-L3 (1:1,000 dilution; peptide antibodies [24]) and ubiquitin (1:500; DakoCytomation, Glostrup, Denmark) in PBS containing 1% BSA. Sections were then incubated for 1 h with biotin-conjugated anti-rabbit IgG diluted 1:200 in PBS, followed by

Vectorstain ABC-PO (Vector Laboratories, Burlingame, CA) for 30 min at room temperature. Sections were developed using 3,3'-diaminobenzidine and counterstained with hematoxylin.

In situ apoptosis was detected by TUNEL (TdT-mediated nick end-labeling) staining with the DeadEnd Fluorometric TUNEL system (Promega, Madison, WI) according to the manufacturer's instructions, to identify apoptotic cells in situ via specific labeling of nuclear DNA fragmentation. Quantification was performed using four mice on each of postoperative days 0, 2 and 4. The total number of apoptotic cells was determined by counting the positively stained nuclei in each caput epididymis section [9]. Four sections from each mouse and 100 total circular tubules per group were processed.

Western blotting

Western blots were performed as previously reported [24]. Total protein (10 μg/lane) from each epididymal region including spermatozoa was subjected to SDS-polyacrylamide gel electrophoresis using 15% gels (Perfect NT Gel, DRC, Japan). Proteins were electrophoretically transferred to polyvinylidene difluoride membranes (Bio-Rad, Hercules, CA) and blocked with 5% non-fat milk in TBS-T (50 mM Tris base, pH 7.5, 150 mM NaCl, 0.1% (w/v) Tween-20). The membranes were incubated individually with primary antibodies to monoubiquitin (1:1,000; u5379, Sigma-Aldrich, St. Louis, MO), UCH-L1 and UCH-L3 (1:1,000 dilution; anti-peptide antibodies [24]), p53, Bax, and Bcl-xL (1:1,000 dilution; all from Cell Signaling Technology, Beverly, MA), and Bcl-2 (1:500; Transduction Laboratories, Franklin Lakes, NJ). Blots were further incubated with peroxidase-conjugated goat anti-mouse IgG or goat anti-rabbit IgG (1:5,000 dilution; Pierce, Rockford, IL) for 1 h at room temperature. Immunoreactions were visualized using SuperSignal West Dura Extended Duration Substrate (Pierce) and analyzed using a ChemiImager (Alpha Innotech, San Leandro, CA). Each protein level was normalized to α-tubulin following analysis with a ChemiImager using AlphaEase software.

Statistical analysis

The mean and standard deviation were calculated for all data (presented as mean ± SD). Student's *t*-test was used for statistical analysis.

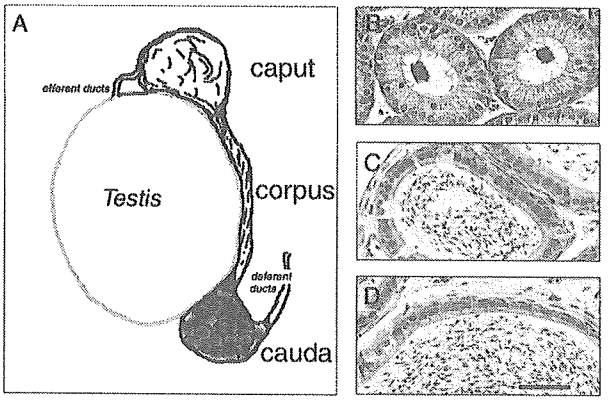

Fig. 1. A: Diagram of the epididymis. B–D: Morphology of the caput (B), corpus (C) and cauda (D) epididymidis from a wild-type mouse. Magnification, 200×. *Scale bar*, 40 μm.

Results

Levels of UCH-L1 and UCH-L3 in individual epididymal regions

The epididymis is a single long, coiled tubule situated on the surface of the testis (Fig. 1A). The epididymal epithelium is composed of four major cell types, principal cells, basal cells, clear cells and narrow cells [7], and can be divided anatomically and functionally into three regions, the caput, corpus and cauda epididymis (Fig. 1B, C, D). We used western blotting to characterize UCH-L1 and UCH-L3 levels along the epididymis (Fig. 2). In wild-type mice, the level of UCH-L1 was highest in the caput epididymis and that of UCH-L3 was highest in the cauda epididymis. UCH-L1 and UCH-L3 were not observed in *gad* and *Uchl3* knockout mice, respectively (Fig. 2; comparison of UCH-L1 and UCH-L3 levels with those in wild-type control mice).

Immunohistochemistry of UCH-L1, UCH-L3 and ubiquitin in the epididymis

Under light microscopy, granular and diffuse UCH-L1 and UCH-L3 immunoreactivity was detected in many epithelial cells of the caput, corpus and cauda epididymis in wild-type mice (Fig. 3A, C). Granular immunoreactivity to ubiquitin was seen in the epithelial cells of the epididymis (Fig. 3B). The distribution of ubiquitin in the corpus and cauda epididymal epithelial cells was similar to that of the caput epididymis,

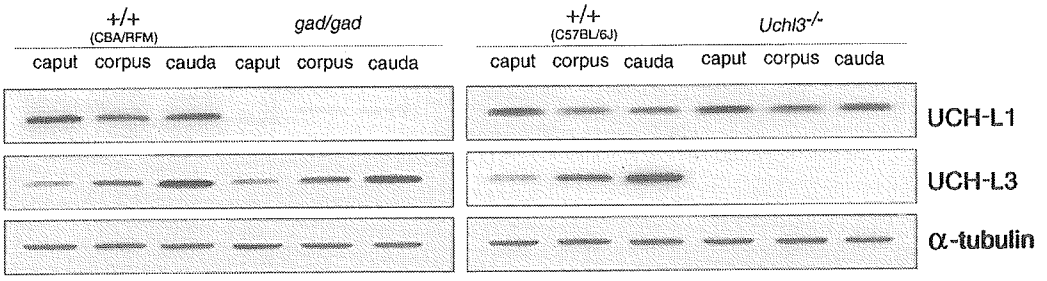

Fig. 2. Comparison of UCH-L1 and UCH-L3 expression by western blotting of caput, corpus and cauda epididymis lysates from two wild-type (CBA/RFM and C57BL/6J), *gad* and *Uchl3* knockout mice. Blots were reprobed for α-tubulin, which was used to normalize the protein load. Images are representative of four independent experiments.

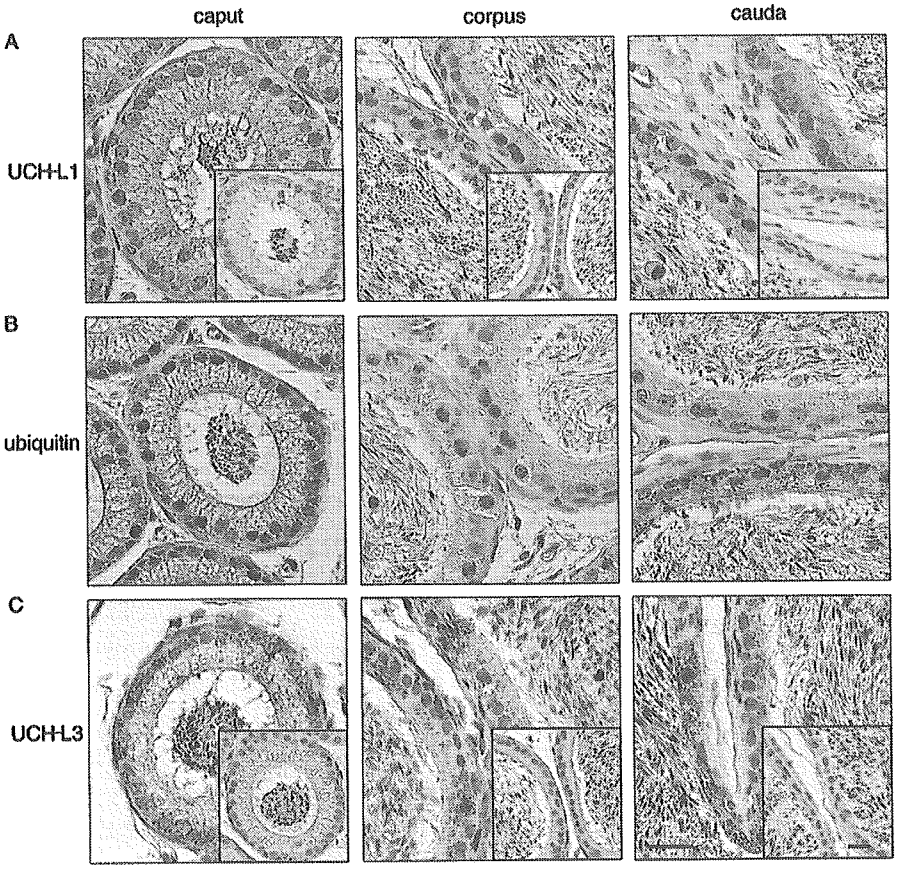

Fig. 3. Immunohistochemistry of UCH-L1, UCH-L3, and ubiquitin in the individual epididymal regions of wild-type mice. Each of the protein-positive cells in the caput, corpus and cauda epididymis is stained by DAB. The insets show that no cells are positive for UCH-L1 and UCH-L3 in the individual epididymal compartments from *gad* (A) and *Uchl3* knockout (C) mice, respectively. A: UCH-L1-positive cells. B: Ubiquitin-positive cells. C: UCH-L3-positive cells. Magnification, 400×. *Scale bar*, 20 μm.

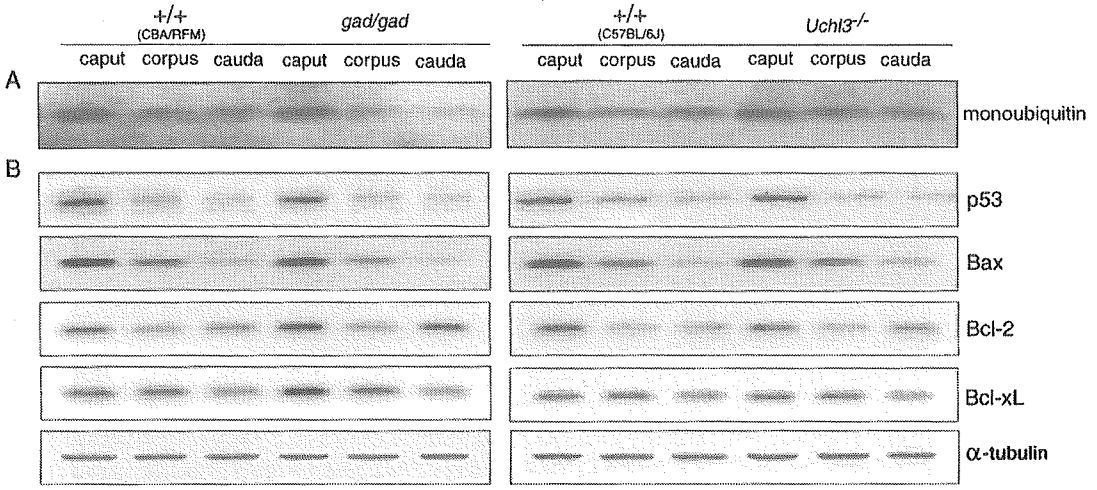

Fig. 4. Western blot analyses showing monoubiquitin and apoptotic proteins in the individual epididymal regions. Total protein (10 μg per lane) was prepared from the caput, corpus and cauda epididymidis from two wild-type (CBA/RFM and C57BL/6J), *gad* and *Uchl3* knockout mice. The blots show the expression levels of monoubiquitin (A) and apoptotic proteins (p53 and Bax) and antiapoptotic proteins (Bcl-2 and Bcl-xL) (B). Blots were reprobed for a-tubulin, which was used to normalize the protein load. Images are representative of four independent experiments.

the ubiquitin staining in these epididymal regions was less intense (Fig. 3B). Immunoreactivity to both UCH-L1 and ubiquitin was intense in the caput epididymal epithelial cells, which was consistent with the expression level (Fig. 2 and Fig. 4A). Diffuse cytoplasmic immunoreactivity in the epididymal epithelial cells to UCH-L3 was intense in the cauda epididymis (Fig. 3C). As shown previously [24], no UCH-L1 or UCH-L3 immunoreactivity was found in the epididymal epithelial cells of *gad* and *Uchl3* knockout mice, respectively (Fig. 3A, C. inset).

Region-specific localization of ubiquitin and apoptotic proteins in the caput epididymis

We previously reported that UCH-L1 binds ubiquitin, and that the level of ubiquitin is decreased in *gad* mice [25, 31]. To determine whether UCH-L1 is associated with the ubiquitin level in the epididymis, we performed western blot analysis of the individual epididymal regions. The monoubiquitin level was markedly higher in the caput epididymis than in the corpus and cauda epididymis, and the low level of monoubiquitin in *gad* mice is consistent with our previous report [25] (Fig. 4A). The epididymis of *Uchl3* knockout mice did not show a difference in ubiquitin level compared with the corresponding wild-type controls.

To explore whether apoptotic phenomenon of spermatozoa in the caput epididymis is in accord with the high expression of apoptotic proteins, we used western blot analysis to verify the expression levels of p53 and Bcl-2 family proteins, which are associated with cell death [12, 28, 29]. The levels of p53 and Bax protein, considered to be proapoptotic, were strikingly high in the caput epididymis, consistent with the pattern of the monoubiquitin level (Fig. 4B). In the *gad* mouse, the levels of the antiapoptotic proteins, Bcl-2 and Bcl-xL, were markedly elevated compared in wild-type mice in the caput epididymis [23] as well as a possible increase in the corpus and cauda epididymis, whereas the levels of apoptotic proteins, p53 and Bax, were unchanged (Fig. 4B). However, we did not detect a difference in the analyzed protein levels between the epididymis of *Uchl3* knockout and wild-type mice.

Region-specific apoptosis in the epididymis following unilateral efferent duct ligation

Androgen deprivation by efferent duct ligation induces glandular epithelial cell death via an apoptotic mechanism [9, 38]. We previously showed that germ cell apoptosis differs between *gad* and *Uchl3* knockout mice following cryptorchid injury [25]. To detect apoptosis in the epididymis following efferent duct li-

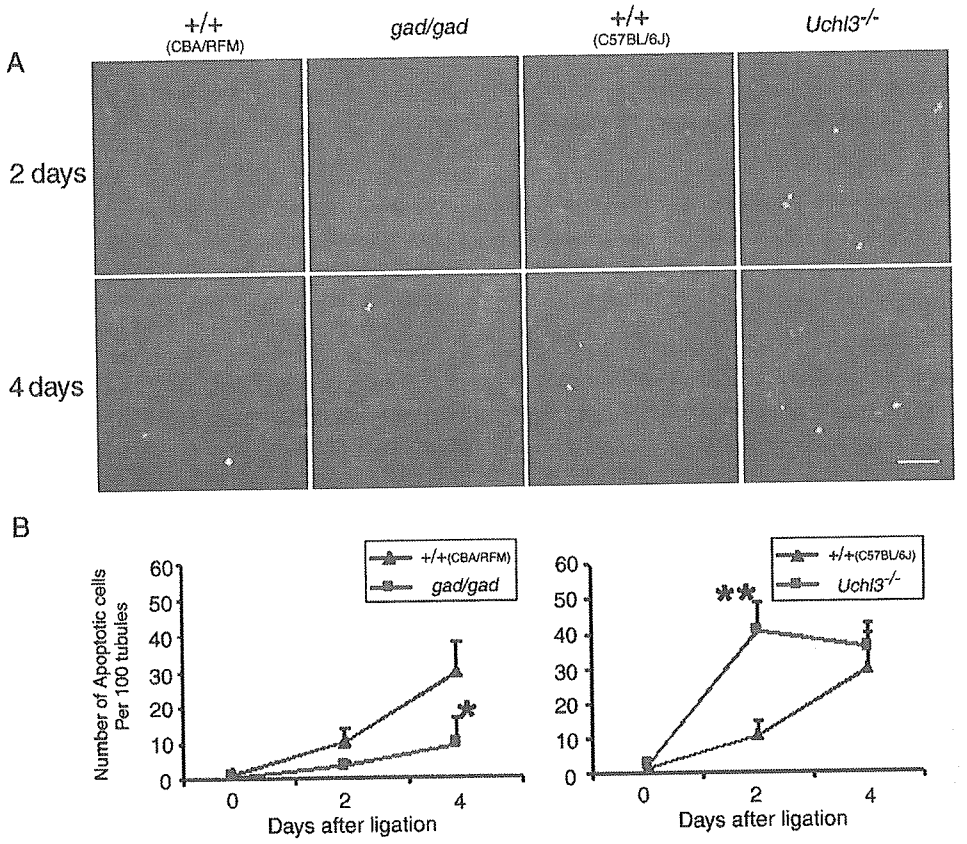

Fig. 5. TUNEL staining of apoptotic cells in the caput epididymis following unilateral efferent duct ligation. A: TUNEL staining in the caput epididymis cross-sections on days 2 and 4 after ligation. Green fluorescence, TUNEL-positive cells; red fluorescence, nuclei stained with propidium iodide. Magnification, 200×. *Scale bar*, 30 μm. B: Quantitation of epithelial cell apoptosis in the caput epididymis following efferent duct ligation. The number of apoptotic epithelial cells in *gad* and wild-type mice is shown on the left. Each value represents the mean ± SD; **P*<0.05. The number of apoptotic epithelial cells in *Uchl3* knockout and wild-type mice is shown on the right. Each value represents the mean ± SD; ***P*<0.01.

gation, we used an *in situ* TUNEL assay to examine apoptosis in *gad* and *Uchl3* knockout mice on postoperative days 2 and 4 (Fig. 5). After efferent duct ligation, epithelial cell apoptosis was observed only in the caput epididymis (mostly the initial segment). The caput epididymis showed a time-dependent increase in epithelial cell apoptosis after efferent duct ligation and epithelial cell apoptosis was found mainly in the principal cells (Fig. 5A). Compared with wild-type mice, the caput epididymis of *Uchl3* knockout mice showed a marked increase in apoptotic epithelial cells on postoperative day 2, whereas *gad* mice resisted efferent duct-ligated epithelial cell apoptosis (Fig. 5A). By postoperative day 2, the number of apoptotic cells per 100 tubules increased with statistical significance (***P*<0.01, *n*=4) in the caput epididymis of *Uchl3* knockout mice as compared with wild-type mice (Fig. 5B). However, *gad* mice showed resistance to ligation-induced apoptosis in the caput epididymis relative to wild-type mice by postoperative day 4 (**P*<0.05, *n*=4) (Fig. 5B).

Discussion

After leaving the testis via the testicular rete, spermatozoa collect in the epididymis, where they undergo final maturation and storage [2, 36, 37]. During epididymal passage, ubiquitination may trigger apoptotic mechanisms that recognize and eliminate abnormal sper-

matozoa, and ubiquitination is believed to play an important role in controlling sperm quality to ensure the production of intact, functional spermatozoa [10, 27, 37]. Ubiquitination of abnormal spermatozoa predominantly occurs in the caput epididymis [37].

Previous studies have shown that two closely-related UCH isozymes, UCH-L1 and UCH-L3 have distinct expression patterns during spermatogenesis [24] and reciprocal functions following cryptorchid injury [25]. We have proposed that UCH-L1 might function as a regulator of apoptosis. Indeed, UCH-L1-deficient *gad* mice are resistant to apoptotic stress [13, 23, 25], and this apoptotic resistance leads to alterations in sperm motility and morphology as well as an increased number of defective spermatozoa in the epididymis of *gad* mice [23]. Our present study demonstrated that UCH-L1 and UCH-L3 have distinct expression patterns along the epididymis in wild-type mice (Fig. 2). We detected a high level of UCH-L1 in the caput epididymis, the main maturation organ, whereas the UCH-L3 level was high in the cauda epididymis, the main storage organ [10]. These region-specific variations in UCH-L1 and UCH-L3 level suggest that they have different functions in the epididymis. The regional differentiation of the epididymis, as suggested by region-specific gene expression, reflects different luminal environments between the regions [16, 19].

We also determined the expression pattern/level of the major component of the proteolytic pathway, ubiquitin, which has specificity for UCH-L1. UCH-L1 associates with monoubiquitin [31], and the monoubiquitin level is reduced in *gad* mice relative to wild-type mice [25, 31]. Predictably, monoubiquitin expression pattern showed similar patterns to UCH-L1 and the monoubiquitin level was reduced in the epididymis of *gad* mice, which had its highest level in the caput epididymis relative to the corpus or cauda epididymis in wild-type mice (Figs. 3 and 4A). Ubiquitin induction is important for regulating programmed cell death, which is a fundamental component of spermatogenesis [1, 23, 32]. Under specific circumstances, the caput epididymis contains a high level of ubiquitin, which may serve to maintain apoptotic mechanisms that eliminate abnormal spermatozoa [37]. This is consistent with the high levels of apoptotic p53 and Bax observed in the caput epididymis compared with the corpus and cauda epididymis (Fig. 4B). Protein p53 and Bax are classically thought to be involved in regulating apoptotic processes, and are targets for ubiquitination [5, 7, 29, 30]. The role of p53 in mediating apoptosis in the male genital tract has been demonstrated in several mice lines [28, 29, 42]. However, p53-independent apoptosis is suggested in the prostate and seminal vesicles by androgen withdrawal or in the rat epididymis by deprivation of luminal factors [3, 11, 14, 38]. Previous studies indicated that Bcl-2 family proteins are involved in the induction or prevention of apoptosis [12, 33, 39, 40]. In *gad* mice, in the present study, the levels of the antiapoptotic proteins, Bcl-2 and Bcl-xL, were markedly increased in the caput epididymis (Fig. 4B), although there was no difference in the levels of the apoptotic proteins, p53 and Bax, relative to wild-type mice. The high levels of Bcl-2 and Bcl-xL in the caput epididymis of *gad* mice is consistent with a previous report that the percentage of morphologically abnormal spermatozoa is significantly higher in *gad* mice [23]. Therefore, the variations of in the levels of Bax, and Bcl-2 and Bcl-xL combined in the caput epididymis probably maintain the regulation of apoptosis [4].

Our previous work focused on the reciprocal functions that UCH-L1 and UCH-L3 exhibit, a distinct feature in testicular germ cells following cryptorchid-induced apoptosis [25]. To characterize the distinct functions of UCH-L1 and UCH-L3 in the epididymis, *gad* and *Uchl3* knockout mice were examined after efferent duct ligation. The epididymal epithelium of the two mutant mice showed differences in apoptotic induction following efferent duct ligation (Fig. 5), after which the circulating androgen level decreases rapidly as a result of apoptotic cell death [9, 20, 38]. After duct ligation, the number of apoptotic cells increased in the caput epididymis of *Uchl3* knockout mice compared with wild-type mice, whereas *gad* mice showed relative resistance in this regard (Fig. 5B). In *gad* mice, the resistance to apoptotic stress can be explained by the high levels of Bcl-2 and Bcl-xL combined in the caput epididymis (Fig. 4B). The tissue androgen level is higher in the caput epididymis than in the corpus or cauda epididymis [15, 38]; thus, apoptotic cells showed in the caput epididymis rather than in the corpus and cauda epididymis following efferent duct ligation. These results may suggest that UCH-L1 and UCH-L3 have reciprocal functions in the caput epididymis fol-

lowing apoptotic stress induced by androgen withdrawal, as was shown with cryptorchid stress [25].

We cannot explain the profound apoptotic phenomenon observed in the present study in the caput epididymis of *Uchl3* knockout mice after efferent duct ligation by the balance of the Bcl-2 family proteins alone. Although our previous report showed that the Nedd8 expression level increased in the testis of *Uchl3* knockout mice [25], we found no difference in the present study (data not shown). The mechanism with regard to the antiapoptotic function of UCH-L3 requires further study. Our present study demonstrated that UCH-L1 and UCH-L3 have distinct expression levels along the epididymis as well as reciprocal functions in response to apoptotic stress induced by androgen withdrawal.

Acknowledgments

We thank H. Kikuchi for technical assistance with tissue sections, and M. Shikama for the care and breeding of animals.

Grant support: This work was supported by Grants-in-Aid for Scientific Research from the Ministry of Health, Labour and Welfare of Japan, Grants-in-Aid for Scientific Research from the Ministry of Education, Culture, Sports, Science and Technology of Japan, a grant from the Pharmaceuticals and Medical Devices Agency of Japan, and a grant from Japan Science and Technology Agency. This paper was supported (in part) by research funds of Chonbuk National University in 2005.

References

1. Baarends, W.M., van der Laan, R., and Grootegoed, J.A. 2000. Specific aspects of the ubiquitin system in spermatogenesis. *J. Endocrinol. Invest.* 23: 597–604.
2. Bedford, J.M. 1979. pp. 7–21. *In*: Evolution of the sperm maturation and sperm storage functions of the epididymis,The Spermatozoon (Bedford DWFaJM, ed). Urban and Schwarzenberg Inc., Baltimore-Muunich.
3. Berges, R.R., Furuya, Y., Remington, L., English, H.F., Jacks, T., and Isaacs, J.T. 1993. Cell proliferation, DNA repair, and p53 function are not required for programmed death of prostatic glandular cells induced by androgen ablation. *Proc. Natl. Acad. Sci. USA.* 90: 8910–8914.
4. Borner, C. 2003. The Bcl-2 protein family: sensors and checkpoints for life-or-death decisions. *Mol. Immunol.* 39: 615–647.
5. Chipuk, J.E. and Green, D.R. 2004. Cytoplasmic p53: Bax and Forward. *Cell Cycle* 3: 429–431.
6. Cooper, T.G. 1998. pp. 602–609. *In*: Epididymis, Encyclopedia of Reproduction (Neil EKaJD, ed). Academic Press Inc., San Diego.
7. Dimmeler, S., Breitschopf, K., Haendeler, J., and Zeiher, A.M. 1999. Dephosphorylation targets Bcl-2 for ubiquitin-dependent degradation: a link between the apoptosome and the proteasome pathway. *J. Exp. Med.* 189: 1815–1822.
8. Ezer, N. and Robaire, B. 2003. Gene expression is differentially regulated in the epididymis after orchidectomy. *Endocrinology* 144: 975–988.
9. Fan, X. and Robaire, B. 1998. Orchidectomy induces a wave of apoptotic cell death in the epididymis. *Endocrinology* 139: 2128–2136.
10. Fraile, B., Martin, R., De Miguel, M.P., Arenas, M.I., Bethencourt, F.R., Peinado, F., Paniagua, R., and Santamaria, L. 1996. Light and electron microscopic immunohistochemical localization of protein gene product 9.5 and ubiquitin immunoreactivities in the human epididymis and vas deferens. *Biol. Reprod.* 55: 291–297.
11. Furuya, Y., Lin, X.S., Walsh, J.C., Nelson, W.G., and Isaacs, J.T. 1995. Androgen ablation-induced programmed death of prostatic glandular cells does not involve recruitment into a defective cell cycle or p53 induction. *Endocrinology* 136: 1898–1906.
12. Gross, A., McDonnell, J.M., and Korsmeyer, S.J. 1999. BCL-2 family members and the mitochondria in apoptosis. *Genes. Dev.* 13: 1899–1911.
13. Harada, T., Harada, C., Wang, Y.L., Osaka, H., Amanai, K., Tanaka, K., Takizawa, S., Setsuie, R., Sakurai, M., Sato, Y., Noda, M., and Wada, K. 2004. Role of ubiquitin carboxy terminal hydrolase-L1 in neural cell apoptosis induced by ischemic retinal injury *in vivo*. *Am. J. Pathol.* 164: 59–64.
14. Jara, M., Esponda, P., and Carballada, R. 2002. Abdominal temperature induces region-specific p53-independent apoptosis in the cauda epididymidis of the mouse. *Biol. Reprod.* 67: 1189–1196.
15. Jean-Faucher, C., Berger, M., Gallon, C., de Turckheim, M., Veyssiere, G., and Jean, C. 1986. Regional differences in the testosterone to dihydrotestosterone ratio in the epididymis and vas deferens of adult mice. *J. Reprod. Fertil.* 76: 537–543.
16. Jervis, K.M. and Robaire, B. 2001. Dynamic changes in gene expression along the rat epididymis. *Biol. Reprod.* 65: 696–703.
17. Jervis, K.M. and Robaire, B. 2002. Changes in gene expression during aging in the Brown Norway rat epididymis. *Exp. Gerontol.* 37: 897–906.
18. Kirchhoff, C. 1998. Molecular characterization of epididymal proteins. *Rev. Reprod.* 3: 86–95.
19. Kirchhoff, C. 1999. Gene expression in the epididymis. *Int. Rev. Cytol.* 188: 133–202.
20. Knorr, D.W., Vanha-Perittula, T., and Lipsett, M.B. 1970. Structure and function of rat testis through pubescence. *Endocrinology* 86: 1298–1304.
21. Kurihara, L.J., Semenova, E., Levorse, J.M., and Tilghman,

S.M. 2000. Expression and functional analysis of Uch-L3 during mouse development. *Mol. Cell. Biol.* 20: 2498–2504.
22. Kwon, J., Kikuchi, T., Setsuie, R., Ishii, Y., Kyuwa, S., and Yoshikawa, Y. 2003. Characterization of the testis in congenitally ubiquitin carboxy-terminal hydrolase-1 (Uch-L1) defective (gad) mice. *Exp. Anim.* 52: 1–9.
23. Kwon, J., Mochida, K., Wang, Y. L., Sekiguchi, S., Sankai, T., Aoki, S., Ogura, A., Yoshikawa, Y., and Wada, K. 2005. Ubiquitin C-Terminal Hydrolase L-1 Is Essential for the Early Apoptotic Wave of Germinal Cells and for Sperm Quality Control During Spermatogenesis. *Biol. Reprod.* 73: 29–35.
24. Kwon, J., Wang, Y.L., Setsuie, R., Sekiguchi, S., Sakurai, M., Sato, Y., Lee, W.W, Ishii, Y., Kyuwa, S., Noda, M., Wada, K., and Yoshikawa, Y. 2004a. Developmental regulation of ubiquitin C-terminal hydrolase isozyme expression during spermatogenesis in mice. *Biol. Reprod.* 71: 515–521.
25. Kwon, J., Wang, Y.L., Setsuie, R., Sekiguchi, S., Sato, Y., Sakurai, M., Noda, M., Aoki, S., Yoshikawa, Y., and Wada, K. 2004b. Two closely related ubiquitin C-terminal hydrolase isozymes function as reciprocal modulators of germ cell apoptosis in cryptorchid testis. *Am. J. Pathol.* 165: 1367–1374.
26. Lippert, T.H., Seeger, H., Schieferstein, G., and Voelter, W. 1993. Immunoreactive ubiquitin in human seminal plasma. *J. Androl.* 14: 130–131.
27. Matin, R., Santamaria, L., Fraile, B., Paniagua, R., and Polak, J.M. 1995. Ultrastructural localization of PGP 9.5 and ubiquitin immunoreactivities in rat ductus epididymidis epithelium. *Histochem. J.* 27: 431–439.
28. Ohta, H., Aizawa, S., and Nishimune, Y. 2003. Functional analysis of the p53 gene in apoptosis induced by heat stress or loss of stem cell factor signaling in mouse male germ cells. *Biol. Reprod.* 68: 2249–2254.
29. Oren, M. 1999. Regulation of the p53 tumor suppressor protein. *J. Biol. Chem.* 274: 36031–36034.
30. Orlowski, R.Z. 1999. The role of the ubiquitin-proteasome pathway in apoptosis. *Cell Death Differ.* 6: 303–313.
31. Osaka, H., Wang, Y. L., Takada, K., Takizawa, S., Setsuie, R., Li, H., Sato, Y., Nishikawa, K., Sun, Y. J., Sakurai, M., Harada, T., Hara, Y., Kimura, I., Chiba, S., Namikawa, K., Kiyama, H., Noda, M., Aoki, S., and Wada, K. 2003. Ubiquitin carboxy-terminal hydrolase L1 binds to and stabilizes monoubiquitin in neuron. *Hum. Mol. Genet.* 12: 1945–1958.
32. Rasoulpour, R.J., Schoenfeld, H.A., Gray, D.A., and Boekelheide, K. 2003. Expression of a K48R mutant ubiquitin protects mouse testis from cryptorchid injury and aging. *Am. J. Pathol.* 163: 2595–2603.
33. Russell, L.D., Chiarini-Garcia, H., and Korsmeyer, S.J., Knudson, C.M. 2002. Bax-dependent spermatogonia apoptosis is required for testicular development and spermatogenesis. *Biol. Reprod.* 66: 950–958.
34. Saigoh, K., Wang, Y.L., Suh, J.G., Yamanishi, T., Sakai, Y., Kiyosawa, H., Harada, T., Ichihara, N., Wakana, S., Kikuchi, T., and Wada, K. 1999. Intragenic deletion in the gene encoding ubiquitin carboxy-terminal hydrolase in *gad* mice. *Nat. Genet.* 23: 47–51.
35. Santamaria, L., Martin, R., Paniagua, R., Fraile, B., Nistal, M., Terenghi, G., and Polak, J.M. 1993. Protein gene product 9.5 and ubiquitin immunoreactivities in rat epididymis epithelium. *Histochemistry* 100: 131–138.
36. Sutovsky, P. 2003. Ubiquitin-dependent proteolysis in mammalian spermatogenesis, fertilization, and sperm quality control: killing three birds with one stone. *Microsc. Res. Tech.* 61: 88–102.
37. Sutovsky, P., Moreno, R., Ramalho-Santos, J., Dominko, T., Thompson, W.E., and Schatten, G. 2001. A putative, ubiquitin-dependent mechanism for the recognition and elimination of defective spermatozoa in the mammalian epididymis. *J. Cell Sci.* 114: 1665–1675.
38. Turner, T.T. and Riley, T.A. 1999. p53 independent, region-specific epithelial apoptosis is induced in the rat epididymis by deprivation of luminal factors. *Mol. Reprod. Dev.* 53: 188–197.
39. Yamamoto, C.M., Sinha Hikim, A.P., Huynh, P.N., Shapiro, B., Lue, Y., Salameh, W.A., Wang, C., and Swerdloff, R.S. 2000. Redistribution of Bax is an early step in an apoptotic pathway leading to germ cell death in rats, triggered by mild testicular hyperthermia. *Biol. Reprod.* 63: 1683–1690.
40. Yang, E., Zha, J., Jockel, J., Boise, L.H., Thompson, C.B., and Korsmeyer, S.J. 1995. Bad, a heterodimeric partner for Bcl-XL and Bcl-2, displaces Bax and promotes cell death. *Cell* 80: 285–291.

Available online at www.sciencedirect.com
SCIENCE DIRECT®
Neuroscience Letters 379 (2005) 149–151
Neuroscience Letters
www.elsevier.com/locate/neulet

Association study of the chemokine, CXC motif, ligand 1 (CXCL1) gene with sporadic Alzheimer's disease in a Japanese population

Yoshiko Tamura[a,1], Yuji Sakasegawa[a,1], Kazuya Omi[a,b], Hitaru Kishida[a,c], Takashi Asada[d], Hideo Kimura[a], Katsushi Tokunaga[b], Naomi S. Hachiya[a], Kiyotoshi Kaneko[a], Hirohiko Hohjoh[a,*]

[a] *National Center of Neurology and Psychiatry, National Institute of Neuroscience, 4-1-1 Ogawahigashi, Kodaira, Tokyo 187-8502, Japan*
[b] *Department of Human Genetics, Graduate School of Medicine, The University of Tokyo, 7-3-1 Hongo, Bunkyo-ku, Tokyo 113-0033, Japan*
[c] *Department of Neurology, Yokohama City University School of Medicine, Yokohama 236-0004, Japan*
[d] *Department of Neuropsychiatry, Institute of Clinical Medicine, University of Tsukuba, Tsukuba 305-8577, Japan*

Received 25 November 2004; received in revised form 21 December 2004; accepted 22 December 2004

Abstract

Inflammation is profoundly involved in the development of Alzheimer's disease (AD) and other neurodegenerative diseases. Chemokine, CXC motif, ligand 1 (CXCL1; or GRO1) is an inflammatory cytokine and appears to be implicated in the pathogenesis of AD. It is of interest and importance to see if the *CXCL1* gene, mapped on chromosome 4q12–q13, has potential for conferring the predisposition to AD. Here we report on an association study of the *CXCL1* gene with sporadic AD patients in a Japanese population; three single nucleotide polymorphisms (SNPs) in the *CXCL1* locus were investigated in 103 AD patients and 130 healthy individuals. The results indicate that neither genotype frequencies nor allele frequencies of the examined SNPs attained statistical significance even after being stratified by the presence or absence of the *Apolipoprotein E ε4* allele. Therefore, the data presented here suggests that the *CXCL1* gene could not be associated with the susceptibility to AD in a Japanese population.

Keywords: Alzheimer' disease; Chemokine; CXC motif, ligand 1 (CXCL1); Single nucleotide polymorphisms (SNPs); Association study

Alzheimer's disease (AD) is a progressive neurodegenerative disorder of the elderly, and characterized by accumulation of neurofibrillary tangles and amyloid deposition resulting in the formation of senile plaques in the brain. Sporadic AD other than familial AD appears to be a multifactorial disorder in which both genetic and environmental factors are involved [2]. A genetic factor strongly associated with sporadic AD has been found in the *Apolipoprotein E* (*APOE*) gene: the *APOE ε4* allele increases the predisposition to AD [10,12,13]. It is likely that other genetic factors besides *APOE ε4* could participate in developing AD, and it is of importance and necessary to determine such genetic factors conferring the predisposition to AD.

Chemokines are inflammatory cytokines which have multiple functions in the immune system, and also have effects on cells of the central nervous system [1,3,4,7–9,15–17]. It appears that inflammation is implicated in the pathogeneses of various neurodegenerative disorders including AD [9,14–17]. Previous study suggested that chemokine, CXC motif, ligand 1 (CXCL1; or GRO1) could work as a potent trigger for the ERK1/2 and PI-3 kinase pathway and induce hypermethylation of the tau protein in mouse primary cortical neurons, and also that the immunoreactivity for CXCL1 increased in a subpopulation of neurons in some AD brains [14]. It was further suggested that a chemokine receptor for CXCL1, CXCR2, was expressed on neurons and was strongly upregulated in a subpopulation of senile plaques in AD [9,15].

* Corresponding author. Tel.: +81 42 342 2711x5176; fax: +81 42 346 1748.
E-mail address: hohjohh@ncnp.go.jp (H. Hohjoh).
[1] These authors contributed equally to this work.

0304-3940/$ – see front matter © 2005 Elsevier Ireland Ltd. All rights reserved.
doi:10.1016/j.neulet.2004.12.056

Table 1
Genotype and allele frequencies of the SNPs in the *CXCL1* locus

SNP name (position[a])		Patients ($n = 103$)	Controls ($n = 130$)	P	OR (95% CI)
rs3117602	Genotype frequency				
(75,199,137)	C/C	90 (87.4%)	107 (82.3%)	0.43	1.0
	C/A	13 (12.6%)	22 (16.9%)		0.7 (0.3–1.5)
	A/A	0 (0%)	1 (0.8%)		–
	Allele frequency				
	C allele	93.7%	90.7%	0.25	
	A allele	6.3%	9.3%		
rs4074	Genotype frequency				
(75,202,395)	G/G	26 (25.2%)	31 (23.8%)	0.95	1.0
	G/A	55 (53.4%)	72 (55.4%)		0.9 (0.45–1.7)
	A/A	22 (21.4%)	27 (20.8%)		1.0 (0.4–2.0)
	Allele frequency				
	G allele	51.9%	51.6%	0.93	
	A allele	48.1%	48.4%		
rs1429638	Genotype frequency				
(75,204,181)	C/C	46 (44.7%)	59 (45.4%)	0.92	1.0
	C/A	51 (49.5%)	65 (50.0%)		1.0 (0.6–1.7)
	A/A	6 (5.8%)	6 (4.6%)		1.3 (0.4–4.2)
	Allele frequency				
	C allele	69.4%	70.2%	0.82	
	A allele	30.6%	29.8%		

[a] The nucleotide positions are based on the numbering used in the NCBI public location.

These observations lead to the possibility that the *CXCL1* gene could confer the predisposition to sporadic AD, i.e., it may be a genetic risk factor for AD, and stimulate our interest in studying if there is any association between the *CXCL1* gene and AD.

In this study, we investigated three single nucleotide polymorphisms (SNPs) around the *CXCL1* locus mapped on 4q12–q13 in sporadic AD patients and healthy individuals. The subjects were all Japanese: 103 patients with AD (47 men and 56 women; mean age of onset, 70.7 years old) were diagnosed by meeting the National Institute of Neurological and communicative Disorders and Stroke and The Alzheimer's Disease and Related Dementias Association criteria (NINCDS-ADRDA) [11], and 130 unrelated healthy individuals (57 men and 73 women; mean age, 70.9 years old) were examined as controls. Peripheral blood samples were obtained and subjected to isolation of genomic DNA with standard protocols. For a high-throughput analysis, allelic discrimination assay with commercially available Assays-on-Demand SNP Genotyping products (Applied Biosystems) was carried out in 25 μl of 1 × TaqMan Universal PCR Master Mix (Applied Biosystems) containing ~10 ng of genomic DNA and 1.25 μl of an Assays-on-Demand SNP Genotyping product (Applied Biosystems) by using the Applied Biosystems 7300 Real Time PCR System (Applied Biosystems) according the manufacture's instructions. The Assays-on-Demand SNP Genotyping products used (the Assay ID numbers; public ID numbers) were as follows: C_9761059_10; rs3117602 (intergenic SNP), C_11820472_1; rs4074 (intron3 SNP), C_2042711_10; rs1429638 (intergenic SNP). The SNPs cover the *CXCL1* gene and the physical distances between rs3117602 and rs4074 SNPs and between rs4074 and rs1429638 SNPs are approximately 3.3 and 1.8 kb long, respectively. After SNP typing, statistical analyses of the data were carried out using SNPAlyse (DYNACOM, Yokohama, Japan). The presence of Hardy-Weinberg equilibrium was examined by χ^2-test for goodness of fit. Allele distributions between the patients and controls were examined by χ^2-test for independence. As for haplotype analysis, haplotype frequencies and linkage disequilibrium parameters were estimated on the basis of an expectation-maximization algorithm [5]. Case–control haplotype analyses were carried out by using the permutation method to obtain the empirical significance [6]. Each haplotype was tested for association by grouping all other haplotypes together and applying χ^2-test with 1 d.f. P values were estimated on the basis of 10,000 replications.

Table 1 shows the results of the SNP typing in the AD patients and healthy controls. The SNPs examined in this study revealed no significant differences in their genotype frequencies, allele frequencies and allele carrier frequencies between the patients and healthy controls. In addition, none of the polymorphisms in each group deviated from expectations based on Hardy-Weinberg equilibrium at a significance level of 0.01. Accordingly, although there was a limitation in the number of the subjects used in this study, i.e., the numbers of the patients and controls used were small; the typing data suggested that the *CXCL1* gene could not be a major risk factor conferring the susceptibility to AD at least. We further examined allelic associations (haplotypes) among the rs3117602, rs4074 and rs1429638 SNPs. As a result, strong

Table 2
Estimated haplotypes and their frequencies

Haplotypes[a]	Patients ($n = 103$), HF (%)	Controls ($n = 130$), HF (%)	P
C–G–C	51.9	50.5	0.75
C–A–A	29.4	28.9	0.66
C–A–C	12.3	11.4	0.75
A–A–C	5.2	7.5	0.32

HF: haplotype frequency.
[a] Estimated haplotypes with the rs3117602, rs4074 and rs1429638 SNPs are indicated and the haplotypes with 5% or more of their frequencies are shown.

allelic associations (haplotypes) among the SNPs were detectable in either the healthy controls or AD patients (Table 2); but, the estimated haplotype frequencies resulted in no significant difference between the patients and controls. We must add that further analyses stratified by either the presence or absence of the *APOE ε4* allele resulted in no statistical significance, although the difference in the frequency of the *APOE ε4* allele alone between the patients and controls attained statistical significance ($P = 0.0079$). Taking all the data together, it is suggested that the *CXCL1* gene is not associated with the susceptibility to sporadic AD. Since inflammation appears to be implicated in the development of AD, it is conceivable that the *CXCL1* gene could contribute to only inflammatory response in the course of the development of AD, but not participate in the pathogenesis of AD as a genetic factor conferring the predisposition to AD.

Acknowledgments

We would like to thank Dr. N. Minami for providing the DNA samples of patients. This work was supported by the Millennium Project of Alzheimer's Disease in Japan.

References

[1] A. Bajetto, R. Bonavia, S. Barbero, T. Florio, G. Schettini, Chemokines and their receptors in the central nervous system, Front Neuroendocrinol. 22 (2001) 147–184.
[2] D. Blacker, L. Bertram, A.J. Saunders, T.J. Moscarillo, M.S. Albert, H. Wiener, R.T. Perry, J.S. Collins, L.E. Harrell, R.C. Go, A. Mahoney, T. Beaty, M.D. Fallin, D. Avramopoulos, G.A. Chase, M.F. Folstein, M.G. McInnis, S.S. Bassett, K.J. Doheny, E.W. Pugh, R.E. Tanzi, Results of a high-resolution genome screen of 437 Alzheimer's disease families, Hum. Mol. Genet. 12 (2003) 23–32.
[3] R. Bonavia, A. Bajetto, S. Barbero, P. Pirani, T. Florio, G. Schettini, Chemokines and their receptors in the CNS: expression of CXCL12/SDF-1 and CXCR4 and their role in astrocyte proliferation, Toxicol. Lett. 139 (2003) 181–189.
[4] C.M. Coughlan, C.M. McManus, M. Sharron, Z. Gao, D. Murphy, S. Jaffer, W. Choe, W. Chen, J. Hesselgesser, H. Gaylord, A. Kalyuzhny, V.M. Lee, B. Wolf, R.W. Doms, D.L. Kolson, Expression of multiple functional chemokine receptors and monocyte chemoattractant protein-1 in human neurons, Neuroscience 97 (2000) 591–600.
[5] L. Excoffier, M. Slatkin, Maximum-likelihood estimation of molecular haplotype frequencies in a diploid population, Mol. Biol. Evol. 12 (1995) 921–927.
[6] D. Fallin, A. Cohen, L. Essioux, I. Chumakov, M. Blumenfeld, D. Cohen, N.J. Schork, Genetic analysis of case/control data using estimated haplotype frequencies: application to APOE locus variation and Alzheimer's disease, Genome Res. 11 (2001) 143–151.
[7] J.K. Harrison, C.M. Barber, K.R. Lynch, cDNA cloning of a G-protein-coupled receptor expressed in rat spinal cord and brain related to chemokine receptors, Neurosci. Lett. 169 (1994) 85–89.
[8] J.K. Harrison, Y. Jiang, S. Chen, Y. Xia, D. Maciejewski, R.K. McNamara, W.J. Streit, M.N. Salafranca, S. Adhikari, D.A. Thompson, P. Botti, K.B. Bacon, L. Feng, Role for neuronally derived fractalkine in mediating interactions between neurons and CX3CR1-expressing microglia, Proc. Natl. Acad. Sci. U.S.A. 95 (1998) 10896–10901.
[9] R. Horuk, A.W. Martin, Z. Wang, L. Schweitzer, A. Gerassimides, H. Guo, Z. Lu, J. Hesselgesser, H.D. Perez, J. Kim, J. Parker, T.J. Hadley, S.C. Peiper, Expression of chemokine receptors by subsets of neurons in the central nervous system, J. Immunol. 158 (1997) 2882–2890.
[10] S.M. Laws, E. Hone, S. Gandy, R.N. Martins, Expanding the association between the APOE gene and the risk of Alzheimer's disease: possible roles for APOE promoter polymorphisms and alterations in APOE transcription, J. Neurochem. 84 (2003) 1215–1236.
[11] G. McKhann, D. Drachman, M. Folstein, R. Katzman, D. Price, E.M. Stadlan, Clinical diagnosis of Alzheimer's disease: report of the NINCDS-ADRDA Work Group under the auspices of Department of Health and Human Services Task Force on Alzheimer's Disease, Neurology 34 (1984) 939–944.
[12] M. Michikawa, K. Yanagisawa, Apolipoprotein E4 induces neuronal cell death under conditions of suppressed de novo cholesterol synthesis, J. Neurosci. Res. 54 (1998) 58–67.
[13] A.M. Saunders, W.J. Strittmatter, D. Schmechel, P.H. George-Hyslop, M.A. Pericak-Vance, S.H. Joo, B.L. Rosi, J.F. Gusella, D.R. Crapper-MacLachlan, M.J. Alberts, et al., Association of apolipoprotein E allele epsilon 4 with late-onset familial and sporadic Alzheimer's disease, Neurology 43 (1993) 1467–1472.
[14] M. Xia, B.T. Hyman, GROalpha/KC a chemokine receptor CXCR2 ligand, can be a potent trigger for neuronal ERK1/2 and PI-3 kinase pathways and for tau hyperphosphorylation—a role in Alzheimer's disease? J. Neuroimmunol. 122 (2002) 55–64.
[15] M. Xia, S. Qin, M. McNamara, C. Mackay, B.T. Hyman, Interleukin-8 receptor B immunoreactivity in brain and neuritic plaques of Alzheimer's disease, Am. J. Pathol. 150 (1997) 1267–1274.
[16] M.Q. Xia, B.J. Bacskai, R.B. Knowles, S.X. Qin, B.T. Hyman, Expression of the chemokine receptor CXCR3 on neurons and the elevated expression of its ligand IP-10 in reactive astrocytes: in vitro ERK1/2 activation and role in Alzheimer's disease, J. Neuroimmunol. 108 (2000) 227–235.
[17] M.Q. Xia, B.T. Hyman, Chemokines/chemokine receptors in the central nervous system and Alzheimer's disease, J. Neurovirol. 5 (1999) 32–41.

RNAi効果の評価法

～本当にRNAiが起こっているのか？

北條浩彦

RNAiは，今日，簡単な遺伝子機能阻害（遺伝子ノックダウン）方法としてさまざまな研究分野で利用されている．この便利な手法を上手に使いこなすためには，誘導するRNAiの遺伝子発現抑制効果を正しく把握する必要がある．そのために，RNAiの評価方法は重要であり，その効果を正確に測定できるものでなければならない．

はじめに

1998年，二本鎖RNAが誘導する不思議な現象（配列特異的な遺伝子発現の転写後抑制），すなわち，RNA干渉（RNA interference：RNAi）が線虫で発見された[1]．その後RNAiは，線虫をはじめ，ショウジョウバエ，原生動物，脊椎動物，そして植物とさまざまな生物種で観察される保存された現象であることが明らかとなった[2)～5)]．そして，2001年，化学合成した小さな二本鎖RNA（small interfering RNA：siRNA）を使って，ほぼすべての哺乳動物細胞にRNAiを誘導できることが示されてから[6]，RNAiは，その不思議な現象に対する学問的な興味だけでなく，その計り知れない応用面に注目が注がれるようになった．今日，RNAiは，簡単な遺伝子ノックダウン方法としてさまざまな研究分野で利用されている．これは，RNAiのツールとしての簡便性，即効性，そして正確性によるものと実感する．この一般的となったRNAi技術を大いに活用するためにも，その効果を正確に評価することが大切である．本稿では，その評価法について，特に哺乳動物RNAiの評価法について解説する．

1．哺乳動物RNAiの特徴とRNAi効果の評価

哺乳動物RNAiの特徴として，siRNA二量体に依存したRNAi活性がある[7]．これは，同じ遺伝子をターゲットとする異なるsiRNA二量体が，それぞれ異なるレベルのRNAi活性を誘導するというものである．当初この特徴は，ターゲットとなるmRNAの二次構造やそれに結合するタンパク質の影響によるものと考えられていたが，現在では，siRNA自身の配列がそれに大きくかかわっていると考えられている[8)～11)]．したがって，ターゲット遺伝子に対して効果的なRNAiを実現するためには，まず，強いRNAi活性を誘導するようなsiRNA二量体を設計しなければならない．

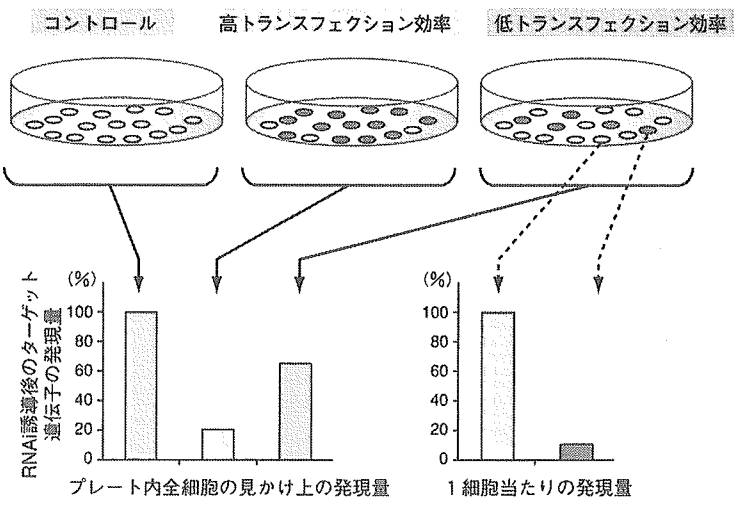

図1●トランスフェクション効率がRNAi評価に与える影響

強いRNAiを誘導するsiRNA二量体（1細胞当たりの発現量）を細胞内にトランスフェクションしたとしても，そのトランスフェクション効率が低いと，ターゲット遺伝子の見かけ上の発現抑制効果は低く評価されてしまう（プレート全体の見かけ上の発現量）．siRNA二量体が導入された細胞を●，何も導入されなかった細胞を○で示してある

今日では，優れたアルゴリズムを備えた予測プログラムによって，そのようなsiRNA二量体を設計することが可能となっている[11)12)]．

さて，そのような強いRNAi活性を誘導するポテンシャルをもったsiRNA二量体を設計できたとしても，実際の細胞内で期待したRNAi効果が誘導できるかどうかは実際にやってみなければわからない．そこで重要になるのが評価法である．評価方法にはさまざまなものがあるが，その戦略から大きく2つに分けることができる．1つは，直接内在性のターゲット遺伝子産物（mRNAやタンパク質）を評価指標とするもの，もう1つは，外因性のレポーター遺伝子を評価指標にするものである．どちらにしても，まず，気を付けなければいけないことは，siRNA二量体を含めた核酸の細胞内導入効率（トランスフェクション効率）である．特に，内在性のターゲット遺伝子産物を直接対象として評価する場合，この導入効率は大きく影響する．図1で示すように，たとえsiRNA二量体が強いRNAi活性を誘導するものであってもトランスフェクション効率が悪かった場合，その後の評価（Q-PCR法*やウエスタンブロット法）で見かけ上の抑制効果は実際よりも低く評価されてしまうのである．それに対して，レポーター遺伝子を用いた評価方法では，レポーターの検出感度に影響が現れるが，レポーターのシグナルが検出可能な範囲内であれば，RNAiの効果を十分評価することができる．

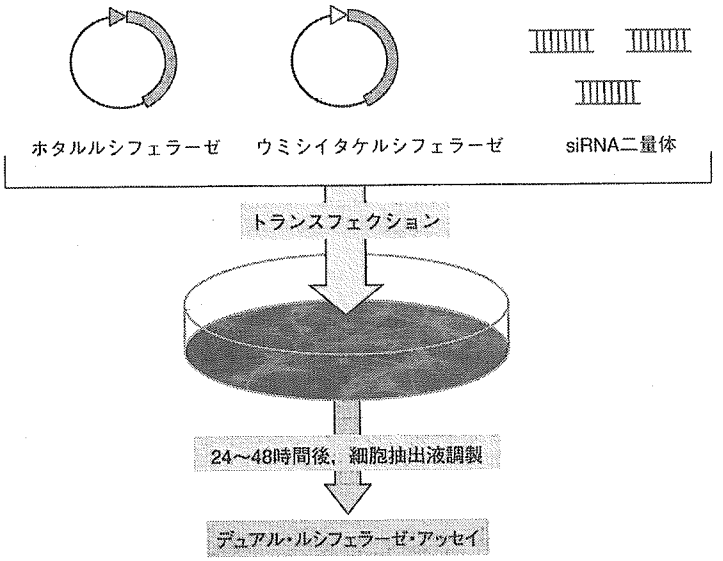

図2●ルシフェラーゼ・レポーター遺伝子を使ったRNAiの評価法

ホタルルシフェラーゼ遺伝子またはウミシイタケルシフェラーゼ遺伝子を含むそれぞれのプラスミドDNAとsiRNA二量体を細胞内に導入（トランスフェクション）する．このとき，ともに導入したsiRNA二量体のターゲットとなるルシフェラーゼ遺伝子がRNAi効果のインディケーターであり，もう片方がコントロール・レポーター遺伝子として測定される．デュアル・ルシフェラーゼ・アッセイを用いて，両者のシグナルを測定し，ターゲット・ルシフェラーゼのシグナル/コントロール・ルシフェラーゼのシグナルで補正し，さらに，何の抑制効果を示さないsiRNA二量体（siControl）を用いて得られた値と比較して，RNAiの効果を評価する

2. レポーター遺伝子を用いたRNAi効果の評価法

レポーター遺伝子を用いたRNAiの評価法には，酵素活性を用いて評価するものと，蛍光タンパク質を用いて評価するものとがある．前者は，ルシフェラーゼ遺伝子に代表されるものであり，後者は，GFP（Green fluorescent protein）

＊Q-PCR（Quantitative-PCR）法
PCR法を用いて，ターゲットDNA量をそのPCR増幅効率から測定する方法．本稿の場合，RNAiを誘導した細胞からRNAを抽出し，それを鋳型に逆転写酵素（reverse transcription：RT）反応によってまずcDNAを合成する．次に，リアルタイムPCR法などを用いてターゲット遺伝子の発現量を測定する．

表1●RNAi評価に用いるレポーター遺伝子の特徴

レポーター遺伝子	レポーターの発現（遺伝子導入後，検出可能な時間）	検出感度	定量性	トランスフェクション効率の影響	生細胞内での検出
酵素系タンパク質（ルシフェラーゼ遺伝子など）	早い（＞約12時間）	◎	◎	ほとんど受けない	△*
蛍光タンパク質（GFP，DsRedなど）	遅い（酵素系と比べて時間がかかる＞24時間）	○	○	受ける場合がある（効率が低いと判定が困難）	◎

◎：優，○：良，△：可
＊ 生細胞用ウミシイタケルシフェラーゼ試薬（Promega）により，生きた細胞内でルシフェラーゼの活性を観察できるようになった

やDsRed（*Discosoma sp.* Red fluorescent protein）遺伝子に代表されるものである．それらの特徴には，それぞれ一長一短があり，それらを表1にまとめてみた．さて，表1からもわかるように，ルシフェラーゼ遺伝子をレポーターに使った評価法は，誘導したRNAi活性，すなわち遺伝子発現抑制効果を簡単に数値化できる点で優れている．そして，多くの研究にこの評価方法が用いられている．これから後半は，ルシフェラーゼ遺伝子を用いた具体的なRNAi評価法について解説する．

ルシフェラーゼ遺伝子を用いたRNAiの評価法は，図2に示すように，2種類のルシフェラーゼ遺伝子を用いて行われる．一般的に，ホタルのルシフェラーゼ（Photinus luciferase）遺伝子とウミシイタケルシフェラーゼ（Renilla luciferase）遺伝子を用いた評価方法が多く利用されている．この2種類のルシフェラーゼは，それぞれ異なる基質要求性があり，これによって同じ反応系であっても基質を変えるだけでそれぞれのルシフェラーゼ活性を区別して測定することができる．実際の実験では，キット化されたデュアル・ルシフェラーゼ定量システムを用いて測定する（図3）．このような評価系では，片方のルシフェラーゼ遺伝子をRNAiのターゲット・レポーター遺伝子，もう一方をコントロール・レポーター遺伝子として解析する．そして，ターゲットのレポーターシグナルをコントロールのレポーターシグナルで補正（正常化）することで実験間のバラツキを小さくし，再現性の高いデータを得ることができる．

この評価システムの利用方法としては，主に2通りある．1つは，機能阻害を目的とする遺伝子に対して設計したsiRNA二量体のRNAi効果を評価する場合，もう1つは，レポーター遺伝子自身をターゲットとするsiRNA二量体を用いてRNAi効果の特徴やメカニズムを解析する場合，さらには改良型または化学修飾したsiRNAのRNAi効果を評価する場合にも利用することができる．プロトコールで，前者のsiRNA二量体

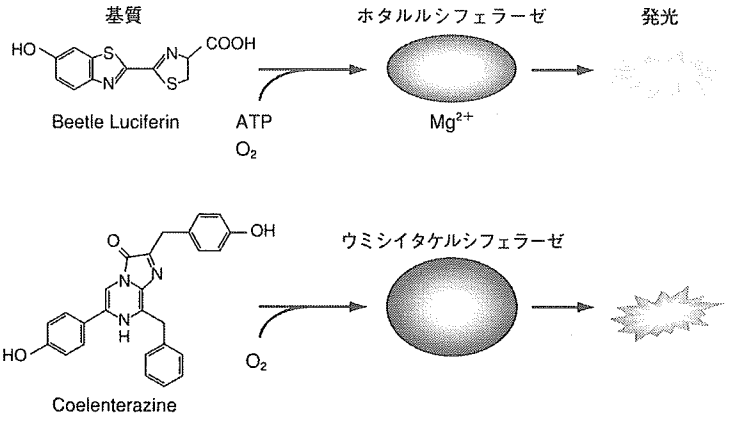

図3●デュアル・ルシフェラーゼ・アッセイのTips

ホタルルシフェラーゼとウミシイタケルシフェラーゼは，それぞれ基質要求性が異なる．前者（ホタル）はBeetle Luciferinを基質とし，後者（ウミシイタケ）はCoelenterazineを基質とする．この基質要求性の違いにより，同一反応系内にそれら二者が存在していても，それらのシグナルを区別して測定することができる．実際の実験（デュアル・ルシフェラーゼ・アッセイ）では，二段階の基質投与によってそれぞれのシグナルを検出する．まず，Beetle Luciferinを基質とした反応で，ホタルルシフェラーゼ活性を測定し，その後直ちに，ホタルルシフェラーゼの失活剤を含むCoelenterazine基質を投入し，ウミシイタケルシフェラーゼの活性を測定する．
測定時の注意点は，比較するサンプル間の基質溶液条件を一定にすることが重要である．これは，Beetle Luciferin基質溶液の保存過程での劣化や，測定前に調製するCoelenterazine基質溶液の調製具合がルシフェラーゼ活性に影響するためであり，測定途中で基質溶液がなくなり新しく調製して測定すると，その前後でシグナルの値が変わり，RNAi活性を正確に比較できなくなる．測定前に，サンプル数＋α分の基質溶液（アッセイ溶液）をまず1つのチューブに調製し，そこから分注することが大切である．

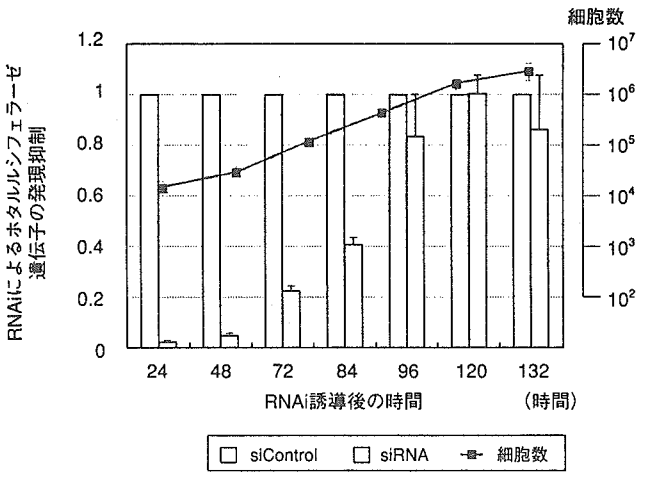

図4●細胞増殖とRNAi効果の持続性

マウスP19細胞に，図2で示した評価系を用いてRNAiを誘導し，その後，RNAi効果の持続性を解析した．この実験では，ホタルルシフェラーゼ遺伝子に対する合成siRNA二量体を使用している．RNAiを誘導して2日ぐらいは強いRNAi効果が観察されるが，その後細胞分裂に伴って，RNAi効果は徐々になくなっていく．これは，siRNA導入によって細胞内に成立した活性型RISC（RNA-induced silencing complex）の一細胞当たりの数が，細胞分裂に伴って減少するためと考えられる（文献13より改変）[13]

プロトコール
psiCHECK™ vectors に siRNA のターゲット配列（合成オリゴ DNA）を挿入したターゲット・レポーター

合成オリゴ DNA 設計のポイント

＊ *Spe* I 制限酵素認識配列を含んだターゲットオリゴ DNA を設計する（右図）．psiCHECK™-1 と psiCHECK™-2 ベクター配列内には *Spe* I 認識配列がないので，この制限酵素を使ってオリゴ DNA が挿入されたポジティブクローンを特定することができる．

＊＊アニーリング後の二本鎖オリゴ DNA の末端が，挿入するベクターの制限酵素切断面に合うように設計する（右図の場合，*Xho* I，*Pme* I 切断面に合うように設計してある）．

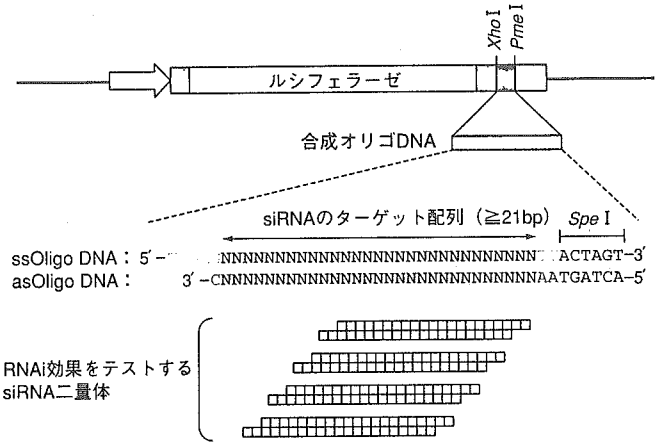

ターゲットオリゴ DNA の設計

1 ターゲット・レポーター遺伝子の作製

● オリゴ DNA のアニーリング

10 × annealing buffer[注1]	1 μl
ssOligo DNA（100 μM）	1 μl
asOligo DNA（100 μM）	1 μl
ddW	7 μl
Total	10 μl

①80 ℃熱変性，5 分間．
②室温にて 30 分間静置．

● ライゲーション

psiCHECK™ Vector（*Xho* I /*Pme* I 消化済）（10 μg/ml）	2 μl
dsOligo DNA（アニーリングしたもの）	1 μl
2 × Ligation Mix（ニッポン・ジーン）	3 μl
Total	6 μl

①16 ℃インキュベーション，30 分間．

● 形質転換

①氷上で，20 μl の JM109 Competent Cells（Promega）にライゲーション反応液 6 μl（全量）を添加する．
②氷上で 30 分間インキュベーション．
③42 ℃，1 分間の熱ショック後，ただちに氷上にて 2 分間静置する．
④S.O.C. Medium（Invitrogen）100 μl を添加する．
⑤LB プレート（100 μg/ml アンピシリンを含む）に播く．
⑥37 ℃インキュベーション，オーバーナイト．

注 1：10 × annealing buffer
・100 mM Tris-HCl（pH 8.0）
・10 mM EDTA
・1 M NaCl

2 簡単ミニプレップ（boiling miniprep）

①形質転換したJM109をLB液体培地（アンピシリンを含む）で培養（37℃，オーバーナイト）.

②1 mlの培養液を1.5 mlチューブにとり，13,000×gで2分間遠心する.

③上清を取除き，菌ペレットに300 μlのSTET溶液[注2]を加え，ボルテックスで懸濁する.

④沸騰したお湯の中にチューブを1分間入れ，その後ただちに氷水に浸けて冷やす（5分間静置）[注3]．このステップで，溶菌とタンパク質変性が起こる.

⑤トップスピードで10分間の遠心.

⑥上清（約200 μl）を新しい1.5 mlチューブに移し，400 μlの100％エタノールを加えて混和させる[注4].

⑦トップスピードで10分間の遠心.

⑧上清を取除き，ペレットを風乾させる.

⑨50 μlのTEに溶解する.

3 制限酵素によるチェック

	（サンプル数15の調整例）	
	×1	×15
10×バッファー	1 μl	15 μl
ddW	6 μl	90 μl
plasmid solution	3 μl	
Spe I[注5]（10units/μl）（TaKaRa）	2U	3 μl
Ribonuclease Mix solution（ニッポン・ジーン）	0.2 μl	3 μl
Total	10 μl	

①37℃インキュベーション.

②アガロース・ゲル電気泳動，EtBr染色によって判定.

③*Spe* Iで消化されたプラスミドがポジティブクローンであり，シークエンスによる最終確認に進む.

4 シークエンス前のプラスミドの精製（PEG沈殿）

①約50 μlのポジティブ・プラスミド溶液に1 μlのRibonuclease Mix solution（ニッポン・ジーン）を添加し，混和させる.

②37℃インキュベーション，30分間.

③30 μlのPEG溶液[注6]を加え，よく混和させる.

④氷上に1時間静置する.

⑤4℃，14 krpm，15分遠心する.

⑥上澄液除去.

⑦～100 μlの75％EtOH（冷凍）で洗い，風乾させる.

⑧20 μlのTEに溶解する.

⑨シークエンス解析または－20℃で保存する.

注2：STET溶液組成
- 8％（wt/vol）Sucrose
- 5％（wt/vol）TritonX-100〔またはポリオキシエチレン（10）オクチルフェニルエーテル，NP-40でも可〕
- 50 mM EDTA
- 50 mM Tris-HCl，pH 8.0

フィルター滅菌後，4℃で保存する．原本（"Current Protocols in Molecular Biology" John Wiley & Sons）では，使用前にリゾチームを加えるようになっているが入れなくてもよい.

注3：
重要なステップである．冷却が不十分な場合，遠心後に大腸菌のゲノムDNAと変性タンパク質がうまくペレットを形成しないため，上清の回収量が減る．このような場合は，ゲノムDNAをチップなどで引っ掛けて取り出し，残った上清に2倍量のエタノールを加える．また，菌数が多すぎても同様な結果になることがあるので注意.

注4：
大腸菌のRNAがキャリアーとなるため，エタノール混和後，ただちに遠心してよい．冷やす必要はない.

注5：
Spe Iと*Nhe* Iのダブル消化でもよい.

注6：PEG溶液組成
- 20％ポリエチレングリコール6000
- 2.5 M NaCl

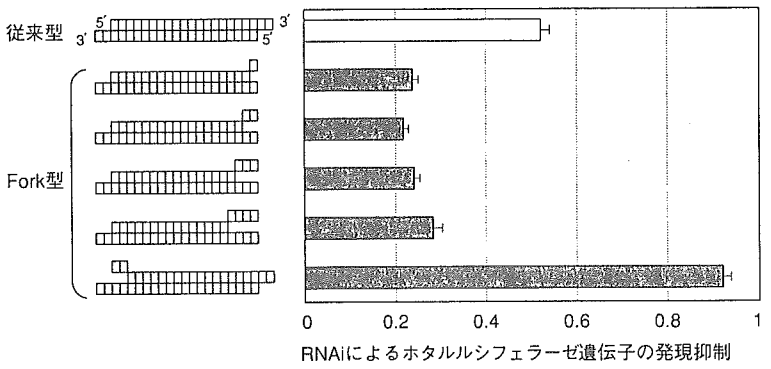

図5●改良型siRNA（Fork-siRNA）二量体によるRNAi効果

siRNAのアンチセンス鎖（RNAiの配列特異的メディエーターとなるsiRNA鎖：赤色のsiRNA鎖）はそのままで，siRNAセンス鎖（水色のsiRNA鎖）の3′末端（または5′末端）にミスマッチ配列を導入しアンチセンス鎖とアニールできなくしたもの．このようなsiRNA二量体は片方の末端が開いた形をとる．このような形状から，"Fork-siRNA duplex"と名づけた．実験では，ホタルルシフェラーゼ遺伝子をターゲットとするsiRNA二量体のさまざまなFork型siRNA二量体を用いてそのRNAi効果を調べた（図2の評価系を使って）．siRNAセンス鎖3′末端にミスマッチを導入するとRNAi効果が高まることが観察された（特許出願中）．おもしろいことに，siRNAセンス鎖5′末端に同様のミスマッチを導入した場合，逆にRNAi効果が失われることが観察された．これらの理由は，Fork型の形状により，Fork末端からの二本鎖RNA，すなわち，siRNA二量体の巻き解きが高まり，それに伴い5′末端から巻き解かれたsiRNA鎖のRISC内取り込みが進むためと考えられる．したがってセンス鎖3′末端にミスマッチを導入した場合，アンチセンス鎖siRNAのRISC取り込みが高まり，その結果，RNAi活性が亢進する．逆に，センス鎖5′末端にミスマッチ配列を導入した場合，センス鎖siRNAのRISC内取り込みが高まり，その結果，ターゲット遺伝子に対するRNAi効果は低下する．これらの結果から，RNAi効果を高めるためには，いかに効率よくアンチセンス鎖のsiRNAをRISC内に取り込ませるかが1つのポイントになると考えられる（文献10より改変）[10]

のRNAi評価に用いるターゲット・レポーター遺伝子の作製について紹介し，図4と図5で，後者のレポーター遺伝子をターゲットとする合成siRNA二量体を使ったRNAi活性の持続性そして改良siRNA二量体を用いたRNAi効果の評価例を紹介する．

3. RNAi評価に利用されるレポーター・プラスミドの種類とその特徴

RNAiに関連するベクターにはさまざまなものがあるが，その大半はsiRNAを細胞内で発現させるためのshRNA（short-hairpin RNA）発現ベクターである．これらのベクターについては，本誌の「目的・方法別siRNAのデリバリー法①～④」を参照していただくこととして，ここではRNAi評価に用いるレポーター・プラスミドについて紹介する．すでに上記で記したように，レポーターを主体とする評価法は，ルシフェラーゼに代表されるような酵素活性を指標にするものと，GFPやDsRedのような蛍光タンパク質を指標にするものとに大別される．実験者は，これらの特徴・性質の違いを十分考慮して（表1），それぞれの実験にあったレポーターを選択することが大切

表2●RNAi評価に用いるレポーターベクター

プラスミド名	pGL3 vectors または PicaGene Vector2	phRL vectors	pGL4 luciferase reporter vectors	psiCHECK™ vectors	蛍光タンパク質発現ベクター pEGFP-N or -Cシリーズベクター，pDsRed2-N1 or -C1ベクター など
メーカー	Promega または ニッポン・ジーン	Promega	Promega	Promega	Clontech Laboratories
レポーター遺伝子	ホタルルシフェラーゼ（改良型）	ウミシイタケルシフェラーゼ（改良型）	ホタル，またはウミシイタケルシフェラーゼ（改良型）	psiCHECK™-1：ウミシイタケルシフェラーゼ psiCHECK™-2：ウミシイタケルシフェラーゼとホタルルシフェラーゼ	Living Colors蛍光タンパク質：EGFP（enhanced GFP） DsRed2（DsRedの変異体）
薬剤耐性遺伝子	*Amp*^{r}	*Amp*^{r}	*Amp*^{r}	*Amp*^{r}	Kan^{r}とNeo^r
特徴・備考	酵素活性を高めるように工夫されたレポーター遺伝子で，一般的なRNAi効果の測定に用いられている．		ルシフェラーゼの高レベル発現と低バックグラウンドを実現したプラスミドベクター．	ウミシイタケルシフェラーゼ遺伝子3′UTRにマルチクローニングサイトがあり，RNAiモニタリング用のターゲット・レポーターを簡単に作製することができる．psiCHECK™-2には，コントロールとなるホタルルシフェラーゼ遺伝子が含まれている．	蛍光の強度を高めるように工夫されている．さらに，哺乳動物細胞内で翻訳効率を高めるためにヒトのコドンに合わせてレポーター遺伝子を最適化している．
測定キット 検出装置	デュアル・ルシフェラーゼ定量システム（Promega）またはPicaGene Dual SeaPansy Luminescence kit（ニッポン・ジーン）など ルミノメーター				蛍光顕微鏡，FACSなど

である．さて，RNAiの活性評価に特化したベクターとしては，Promega社のRNAi効果検定用ルシフェラーゼレポーターベクター，psiCHECK™ vectorsがある．これらのベクターは，ウミシイタケルシフェラーゼ・レポーター遺伝子の3′UTRにマルチクローニングサイトがあり，簡単にターゲット・レポーター遺伝子を作製できるようになっている．さらに，psiCHECK™-2 vectorにはコントロールとなるホタルルシフェラーゼ遺伝子も含んでいるため，1つのプラスミドベクターを用いてターゲットとコントロールの両方を解析できるようになっている．プロトコールを参考にしてターゲット・レポーター・プラスミドを作製し，それらを用いて簡単にRNAiの活性評価，設計したsiRNAのRNAi誘導効果を評価することができる．psiCHECK™ vectors以外にも代表的なレポータープラスミド・ベクターを表2に挙げたので参考にしていただきたい．

おわりに

RNAiは，今日，簡便な遺伝子機能阻害方法として揺るぎない地位を確立したといえる．そして今後，さらに多くの研究・開発に利用されていくと考えられる．この一般的となったRNAi技術を上手く利用するためには，siRNAの設計，siRNAの（目的細胞・組織への）デリバリー，そして誘導したRNAiの活性評価が重要なポイントになると考える．これらのポイントを押さえ，効果的なRNAiを実現し，大いに研究に役立てていただきたいと願う．

参考文献

1）Fire, A. et al.：Nature, 391：806-811, 1998
2）Bosher, J. M. & Labouesse, M.：Nature Cell Biol., 2：E31-36, 2000
3）Fire, A.：Trends Genet, 15：358-363, 1999
4）Sharp, P. A.：Genes Dev., 13：139-141, 1999
5）Vaucheret, H. & Fagard, M.：Trends Genet., 17：29-35, 2001
6）Elbashir, S. M. et al.：Nature, 411：494-498, 2001
7）Hohjoh, H.：FEBS Lett., 521：195-199, 2002
8）Khvorova, A. et al.：Cell, 115：209-216, 2003
9）Schwarz, D. S. et al.：Cell, 115：199-208, 2003
10）Hohjoh, H.：FEBS Lett., 557：193-198, 2004
11）Ui-Tei, K. et al.：Nucleic Acids Res., 32：936-948, 2004
12）Naito, Y. et al.：Nucleic Acids Res., 32：W124-129, 2004
13）Omi, K. et al.：FEBS Lett, 558：89-95, 2004

北條浩彦（Hirohiko Hohjoh）

1990年九州大学大学院医学系研究科博士課程修了．1991年東京大学医科学研究所助手．1992年米国国立衛生研究所（NIH），国立ガン研究所（NCI）生化学研究室研究員．1997年東京大学大学院医学系研究科人類遺伝学教室助手．2002年 国立精神・神経センター神経研究所室長～現在に至る．